Letter

Evolution equation for elastic scattering of hadrons

Hiren Kakkad[a], Anderson Kendi Kohara[b], Piotr Kotko[c]

Faculty of Physics and Applied Computer Science, AGH University Of Science and Technology, Mickiewicza 30, 30-059 Kraków, Poland

Abstract We turn high energy elastic scattering of hadrons into an initial value problem using an evolution equation based on the Regge Field Theory, which has a form of the complex nonlinear reaction–diffusion equation, with time being played by the logarithm of energy. The initial conditions are provided by the data-driven models for the real and imaginary parts of the amplitude. Numerical calculations of pp differential cross sections and forward quantities for LHC energies agree very well with experimental data extending up to, and including the diffractive cone. Furthermore, we show that at current accessible energies the nonlinear effects play an important role, as the impact parameter space profiles approach the unitarity bound. The equation also predicts some other effects discussed in the literature, like the hollowness of nuclear matter or existence of stationary points in momentum transfer t.

1 Introduction

High energy relativistic scattering of hadrons can be classified into two major types: elastic and inelastic. If a large momentum scale is present, the latter can be treated within perturbative Quantum Chromodynamics (QCD) and factorization theorems. The elastic scattering of hadrons, on the other hand, belongs to a non-perturbative domain of QCD, except for very large momentum transfers, where perturbative techniques may be applied. Despite the apparent simplicity of the process, which depends only on two kinematical variables s (the center of mass energy squared) and t (the transferred momentum squared), it is still considered an open problem, as there is no convincing description of elastic scattering in terms of QCD.

At $\sqrt{s} \sim$ few GeV the elastic scattering data can be described relatively well by the Regge phenomenology [1], which represents the scattering amplitude using the partial wave expansion and singularities in the complex l-plane. The linear relation between l and t, called the Regge trajectory, can be attributed to an exchange of family of meson in t channel. However, for large energies (ISR domain and beyond), these regular reggeon linear trajectories fail to describe the rise of the total cross section, as well as the shrinkage of the diffractive cone. Thus, one introduces another effective trajectory with a lower slope and positive intercept. This effective object is the so-called *Pomeron*, a pseudo-particle with isospin zero and even $\mathcal{C}$-parity.

The perturbative QCD predicts the Pomeron as a color singlet composed of two gluons. Its energy evolution is given by the Balitsky–Fadin–Kuraev–Lipatov (BFKL) equation [2–4] (see also [5] for a review), which predicts a power like growth of the gluon density with energy. However, for asymptotic energies, the power growth has to be tamed, due to the Froissart bound based on the unitarity of the scattering matrix and the finiteness of strong interaction range. From the perturbative perspective, the gluon density gets so large that fusion of gluons becomes important, leading to the gluon saturation phenomenon [6]. Saturation can be incorporated in the non-linear extension of the BFKL – the Balitsky–Kovchegov (BK) equation [7–9], which is a mean field approximation to an infinite set of coupled differential equations for Wilson line correlators known as Balitsky–Jalilian–Marian–Iancu–McLerran–Weigert–Leonidov–Kovner (B-JIMWLK) equation [7,10–17].

Despite the fact that these sophisticated QCD evolution equations had a tremendous impact on both theoretical and phenomenological studies of high energy processes, in particular processes not involving hadrons (onium–onium scattering [18]), they are not appropriate to describe elastic scattering experimental data [19]. The perturbative treatment leads to the conformal, impact-parameter-independent evo-

[a] e-mail: kakkad@agh.edu.pl

[b] e-mail: kohara@agfh.edu.pl (corresponding author)

[c] e-mail: pkotko@agh.edu.pl

lution kernel (the b appears only in the Pomeron amplitude in combination with the target transverse size – such b dependent solution was discussed in [20]). The lack of b-space diffusion was recently addressed in [21], but the equations have not been tested phenomenologically.

In this work, we formulate an evolution equation for the *complex* elastic scattering amplitude that successfully describes the data and has some resemblance to the aforementioned perturbative equations. Before we introduce and motivate our equation, let us briefly outline the main concepts. The diffusion in impact parameter space was first discussed by Gribov [22]. In the 60's, he also developed the Reggeon Calculus [23], where the Pomeron was treated as a quasi-particle exchanged in the t channel, which ultimately lead to the formulation of the Regge Field Theory (RFT). In [24–26] a Lagrangian with triple interaction vertex was studied to describe the Pomeron interactions. It is interesting to note that, already in 70', a rapidity evolution equation for the Pomeron correlation functions, preserving diffusion and containing the non-linear quadratic term, was derived in the semi-classical approximation [27]. This equation has a form of the Fisher–Kolmogorov–Petrovsky–Piscounov (FKPP) equation (the reaction–diffusion equation) [28,29], which is known to be related to the QCD BK equation [30]. At that time there were no experimental data at high energies that could utilize the non-linear phenomena encoded in these equations. Nowadays, in the LHC era, the energies involved are adequate not only to study the non-linear phenomena that elastic amplitudes must contain, but also to study more subtle effects coming from inclusion of the Odderon fields and higher order Pomeron couplings. The Odderon is a fundamental prediction of perturbative QCD, which is a color singlet state of gluons with odd parity. Recently, the D0 and Totem collaborations, studying the difference between pp and p̄p cross sections at different energies, concluded that an odd amplitude is necessary to explain the data leading to the possible Odderon discovery at the LHC. [31].

In the present work, based on [27], we derive a nonlinear evolution equation for the complex elastic amplitude and confront it with up-to-date experimental data. The evolution equation is somewhat similar the one presented in Ref. [32], where analytic properties of the solutions to the real FKPP equation with a noise term were investigated, independently of the initial conditions. In our work, on the other hand, we solve the full complex equation, tying together the real and imaginary amplitudes, using the data-driven phenomenological models [33,34] as initial conditions. We show that our complex equation describes the data exceptionally well up to the dip-bump region in the differential elastic cross section as well as the quantities in the forward regime.

2 Evolution equation for elastic amplitude

The relation between the S-matrix and the elastic scattering amplitude reads

$$\mathcal{S}(s,t) = 1 + i\mathcal{T}(s,t), \tag{1}$$

where the transition amplitude $\mathcal{T}$ has real and imaginary parts

$$\mathcal{T} = T_R + iT_I. \tag{2}$$

We define the impact parameter space amplitude as the Fourier transform of the transverse components of the momentum transfer q, $t \simeq -\mathbf{q}^2$,

$$\widetilde{\mathcal{T}}(\tau, \mathbf{b}) = \int d^2\mathbf{q}\, e^{-i\mathbf{b}\cdot\mathbf{q}}\, \mathcal{T}(\tau, -\mathbf{q}^2), \tag{3}$$

where $\tau \simeq \log s$ is the rapidity and the bold symbols represent transverse vectors.

In the Regge theory the energy growth of the amplitude is attributed to the Pomeron exchange:

$$\mathcal{T}(s,t) = g_a(t)\, g_b(t)\, e^{[\alpha_P(t)-1]\log s} \left(i - \cot\frac{\pi\alpha_P(t)}{2}\right), \tag{4}$$

where $\alpha_P(t) = 1 + \epsilon_0 + \alpha' t$ is the standard linear Pomeron trajectory with the intercept ϵ_0 and the slope α'. The functions g_i are the hadronic form factors.

It is easy to check that the b-space amplitude, in the large b limit, satisfies the following diffusion equation

$$\frac{\partial \widetilde{\mathcal{S}}(\tau, \mathbf{b})}{\partial \tau} = \left(\alpha' \nabla_{\mathbf{b}}^2 - \epsilon_0\right) \widetilde{\mathcal{S}}(\tau, \mathbf{b}). \tag{5}$$

Equation (5), however, violates the Froissart bound and, furthermore, its solutions are in contradiction with high energy LHC data. To correct that, we use the RFT approach with the following Lagrangian density [24]

$$\mathcal{L} = \frac{1}{2} p \overleftrightarrow{\partial}_\tau q + \alpha' \nabla_b q \cdot \nabla_b p - \epsilon_0\, p\, q + \lambda\, p\, q\, (p+q), \tag{6}$$

where the fields q and p are related to Gribov's Pomeron fields, $q = i\overline{\Psi}$, $p = i\Psi$ and depend both on b and τ. Above, λ is the triple Pomeron coupling. As pointed out in [25], in addition to the zero energy ground state $|\phi_0\rangle$, the Hamiltonian acquires a non zero energy state $|\phi_1\rangle$, which for large τ and positive intercept ϵ_0 approaches a coherent state. A general τ dependent state is constructed as $|\psi(\tau)\rangle = \exp(-\hat{A}(\tau))|\phi_0\rangle$, where the operator $A(\tau)$ is given by an infinite sum of $(n+1)$-point correlation functions convoluted with the Pomeron creation operators $\hat{q}$:

$$\hat{A}(\tau) = \sum_{n=1}^{\infty} \frac{1}{n!} \int d^2\mathbf{b}_1 ... d^2\mathbf{b}_n \, \hat{q}(\mathbf{b}_1) ... \hat{q}(\mathbf{b}_n) \, G_n(\tau, \mathbf{b}_1, .. \mathbf{b}_n).$$

(7)

Equation (7) inserted to the Schrödinger equation $\partial_\tau |\psi(\tau)\rangle = -H |\psi(\tau)\rangle$, gives an infinite set of coupled differential equations for the correlators G_n. In the semi-classical approximation it reduces to an uncoupled set of equations. In particular, for the two point correlation function one gets [26]

$$\frac{\partial G_1(\tau, \mathbf{b})}{\partial \tau} = \left(\alpha' \nabla_{\mathbf{b}}^2 + \epsilon_0 \right) G_1(\tau, \mathbf{b}) - \lambda G_1(\tau, \mathbf{b})^2.$$

(8)

Since the energy dependence of the elastic amplitude is driven by the one-Pomeron exchange, cf. Eq. (4), the evolution equation for the two-point correlator can be readily transformed into the equation for the amplitude itself and thus the S-matrix. Because hadrons act as sources in RFT, the b-dependent hadron state is simply represented by a coherent state $|p(\mathbf{B})\rangle = \exp(-\int d^2b \, f(\mathbf{b} - \mathbf{B}) \, \hat{q}(\mathbf{b})) |\phi_0\rangle$ with the profile function f peaked around zero. The source function f, together with $G_1(0, \mathbf{b})$, provide the initial conditions and can be complex valued. Putting these ingredients together, we obtain the following equation for the S-matrix

$$\frac{\partial \widetilde{\mathcal{S}}(\tau, \mathbf{b})}{\partial \tau} = \left(\alpha' \nabla_{\mathbf{b}}^2 - \epsilon_0 \right) \widetilde{\mathcal{S}}(\tau, \mathbf{b}) + \lambda \widetilde{\mathcal{S}}(\tau, \mathbf{b})^2.$$

(9)

This equation resembles the FKPP equation [28,29]. However, since $\widetilde{\mathcal{S}}$ is a complex quantity the above equation provides a set of two real coupled differential equations for the real and imaginary amplitudes. An interesting fact is that these two equations

$$\frac{\partial \widetilde{T_I}}{\partial \tau} = \alpha' \frac{\partial^2 \widetilde{T_I}}{\partial b^2} + \epsilon_0 \left[\widetilde{T_I}(1 - \lambda \widetilde{T_I}) + \lambda \widetilde{T_R}^2 \right],$$

(10)

and

$$\frac{\partial \widetilde{T_R}}{\partial \tau} = \alpha' \frac{\partial^2 \widetilde{T_R}}{\partial b^2} + \epsilon_0 \widetilde{T_R} (1 - 2\lambda \widetilde{T_I})$$

(11)

have a very similar structure to the Pomeron and Odderon energy evolution equations of the BK type [30,35].

In order to use the above equations one needs appropriate initial conditions, which specify the impact parameter profile functions for $\widetilde{T_I}$ and $\widetilde{T_R}$, at a given initial energy. Once these are known, for instance, from phenomenological models/parametrizations, they provide both the energy dependence and impact parameter evolution of the amplitudes at any energy.

Equation (9) is derived solely from the triple-Pomeron interactions within the RFT, and as discussed before, does not include the Odderon fields and higher order Pomeron couplings in the evolution (it may include them however,

indirectly, in the initial condition, as both real and imaginary parts have to be provided). Nevertheless, Eq. (9) captures the key elements of the experimental data when supplied with appropriate initial profiles, leaving space for inclusion of the Odderon fields and other higher order non-linear terms.

3 Numerical results

In this section we solve the nonlinear equation (9), equivalent to the set of Eqs. (10)–(11), numerically and confront it with the existing pp elastic scattering data. Moreover, we provide predictions for energies not accessible today, but likely to be explored by the future particle colliders or cosmic ray experiments.

In our normalization the differential cross section reads:

$$\frac{d\sigma}{dt} = \pi \, (\hbar c)^2 \Big[T_I(s, t)^2 + T_R(s, t)^2 \Big],$$

(12)

where $(\hbar c)^2 = 0.389379$ mb GeV^2. For the sake of simplicity, in our analysis we disregard the Coulomb interaction and consequently its interference with the nuclear amplitude. The forward quantities, obtained in the limit of $t = 0$, include the total cross section σ_{tot} via the optical theorem, the ratio ρ of the real and imaginary parts, and the imaginary and real slopes B_I, B_R. These are defined respectively as follows:

$$\sigma_{\mathrm{tot}} = 4 \pi \, (\hbar c)^2 \, T_I(s, 0),$$

(13)

$$\rho = \frac{T_R(s, 0)}{T_I(s, 0)},$$

(14)

$$B_{I,R} = \frac{2}{T_{I,R}(s, t)} \frac{dT_{I,R}(s, t)}{dt} \bigg|_{t=0}.$$

(15)

The initial conditions for the differential equation have to be set up by a measurement at lower energies through extracted b-space profiles, both for the real and imaginary parts. In the present work we use the Kohara–Ferreira–Kodama (KFK) model [33,36], and independently the Bourrely–Soffer–Wu (BSW) model [34] to test the initial condition dependence of the predictions. The main advantage of these models is that they possess analytic forms in b-space.

It is important to stress that the initial conditions require b-space profiles at certain fixed initial energy. Our phenomenological studies show that our evolution equation is suitable for large energies (beyond ISR). We observe that the real part of the evolution equation is monotonically reduced with the increasing energy, which, consequently, causes a reduction in the ρ parameter. Therefore, we choose to start with the initial condition at $\sqrt{s} = 500$ GeV, since at this energy, according to the dispersion relations expectations for a given total cross section parametrization (see PDG [37]), the ρ value should be close to its maximum.

Table 1 The parameters α', ϵ_0 and λ are presented separately for the KFK and the BSW initial conditions

	α' (GeV^{-2})	ϵ_0	λ
KFK	0.105	0.129	0.712
BSW	0.090	0.140	0.820
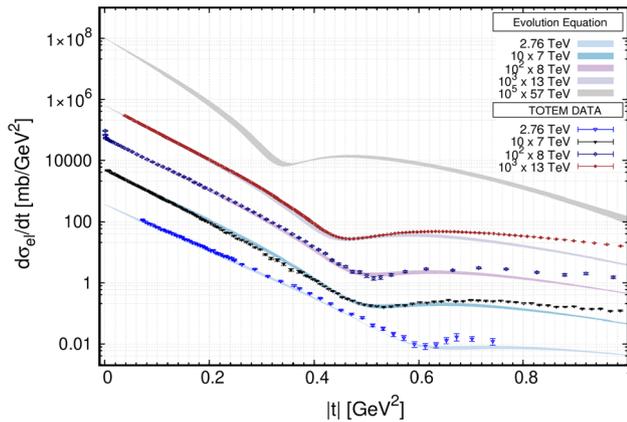
Fig. 1 The points represent the TOTEM proton-proton elastic differential cross-section measured at 2.76. 7, 8 and 13 TeV with statistical uncertainties (bars) in the $|t|$ range $0 < |t| < 1$ GeV^2. The colored bands represent the predictions made using the coupled non-linear evolution equation Eqs. (10), (11) for the KFK and BSW b-space initial profiles

In Table 1 we show the parameters of the evolution equation, α', ϵ_0 and λ, determined in such a way that our solution-based differential cross-section – for some higher energy, in our case 7 TeV – fits the experimental data. These values are rather stable for different initial conditions and used for all other energies. It is remarkable that the Pomeron intercept ϵ_0 is close to the standard nonperturbative intercept $\epsilon_\mathcal{P} = 0.096$. The Pomeron slope (the diffusion coefficient) is close to 0.1 GeV^{-2}, which is below the standard value 0.25 GeV^{-2}, but the possibility of this reduction was predicted in the 70's [38]. We also observe the stability of the triple Pomeron coupling.

For the available LHC energies and low to moderate t we observe a good match between our predictions and the TOTEM data for the differential cross section. The bands shown in Fig. 1 result from the difference in the predictions for the KFK and BSW initial conditions. For a given value of t, the lower limit of the band is defined by the minimum of the predictions for the two initial conditions, while the upper limit is defined by the maximum of the two. For higher values of t, including the dip and the bump regions, the positions and magnitudes also match well with the experimental data. Quantitatively, the calculated dip positions shown in Table 2 are in well agreement with TOTEM measurements. Beyond the bump, our solutions go below the experimental data. Since this region is still far from the perturbative tail in terms of QCD, in our opinion this could be explained with

the inclusion of other interaction terms in the Lagrangian of RFT, which will be investigated in future work.

The real and imaginary amplitudes in the t-space exhibit similar analytic behaviour compared to other models available in the literature [34,36,39,40]. As can be seen in Fig. 2, the real part has the first zero before the zero of the imaginary part. This zero approaches the origin before the zero of the imaginary part with the increasing energy in accordance with the theorem of Martin [41]. On the other hand, the zero of the imaginary part is close to the dip position. The dip structure, i.e. its magnitude and shape, are determined by the interplay of the imaginary and the real part, which is non-zero in this region for several energies.

Another intriguing aspect is the presence of fixed points (stationary points) for various energies in both real and imaginary amplitudes, i.e. the points for which the curves intersect for different energies. The first fixed point in the real part is at $|t| = 0.07$ GeV^2, and the second is at $|t| = 0.5$ GeV^2. For imaginary part, the first fixed point is at $|t| = 0.2$ GeV^2, and the second at $|t| = 1.0$ GeV^2. These fixed points constrain the shape of real and imaginary amplitudes and could indicate the uniqueness of the scattering amplitudes. Although not exactly at the same positions, these fixed points were also observed by Csörgő et al. in Refs. [40,42].

In Table 2 we summarize the standard forward quantities calculated at different energies. For the total cross section σ_{tot}, the obtained values for both initial conditions agree with TOTEM [43] for different energies, and with AUGER [44], whereas for the ATLAS [45,46] data our result seems to be slightly above. For ρ, our results are again substantially within the error limits for the extracted values at 7 and 8 TeV from TOTEM. For 13 TeV, the prediction for KFK initial condition is within the error limits, whereas for BSW the value falls slightly outside the error bar. We believe that the inclusion of the Coulomb interaction might introduce some corrections due to its interplay with the real nuclear part. Interestingly, the measured slope B, which is weighted average between the real B_R and imaginary B_I slopes, is in between the calculated values for both initial conditions.

Although not observable, the b-space profiles are useful to analyze the interaction mechanism. At low energies the diffusive and linear parts of the evolution equation drive the dynamics of the scattering amplitudes. However, at large energies the non-linear effects become important. Due to the presence of the triple Pomeron vertex, the diffusive evolution equation follows a reactive-diffusive system that contains essentially two regions: one for stable solution at large b and another for unstable solution at small b. The LHC energies are especially interesting because the transition from the linear regime to the non-linear can be probed. In this energy range the profiles grow with the energy and eventually reach the unitarity bound (similar to the saturation mechanism for gluons). Once the profiles reach the unitarity bound the only

Table 2 Forward quantities σ_{tot}, ρ, B calculated using both KFK and BSW initial conditions, for various energies. We also show the available experimental data at LHC energies – TOTEM 2.76–13 TeV [43,54–58] (and the references therein), ATLAS 7 and 8 TeV [45,46] – and Cosmic Ray experiment – AUGER [44]. The ρ values for ATLAS are fixed according to COMPETE parametrization [37]

	$\sqrt{s}$ [TeV]	σ_{tot} [mb]	ρ	B [GeV^{-2}]
KFK initial condition	2.76	84.31	0.123	17.28
	7	99.07	0.117	18.47
	8	101.32	0.116	18.65
	13	109.78	0.113	19.32
	57	138.32	0.105	21.55
BSW initial condition	2.76	83.14	0.143	19.69
	7	98.40	0.134	21.12
	8	100.73	0.132	21.34
	13	109.52	0.127	22.15
	57	142.30	0.115	24.87
TOTEM	2.76	84.7 ± 3.3	–	17.1 ± 0.30
	7	98.0 ± 2.5	0.145 ± 0.091	19.73 ± 0.40
	8	101.7 ± 2.9	0.12 ± 0.03	19.74 ± 0.28
	13	110.6 ± 3.4	0.10 ± 0.01	20.40 ± 0.01
ATLAS	7	95.35 ± 0.38	0.14 (fix)	19.73 ± 0.14
	8	96.07 ± 0.18	0.136 (fix)	19.74 ± 0.05
AUGER	57	133 ± 29	–	–
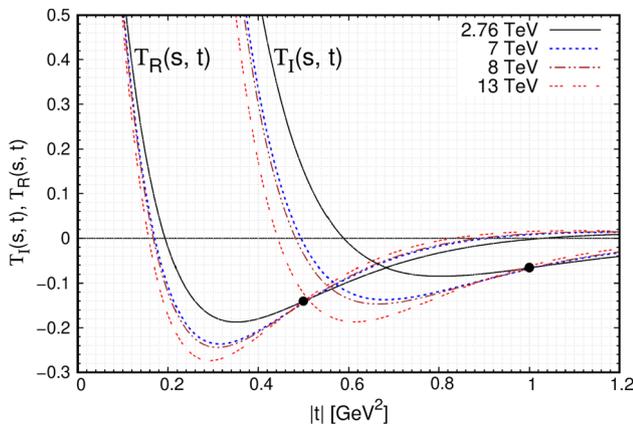
Fig. 2 Real and imaginary pp amplitudes obtained numerically for the KFK initial conditions for the LHC energies
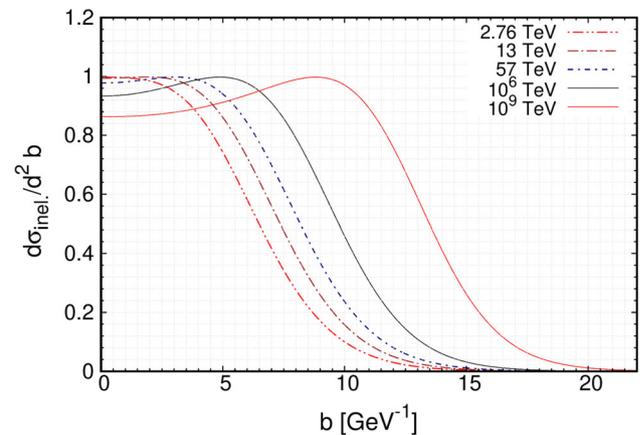
Fig. 3 Inelastic profiles obtained numerically using the evolution equation Eq. (9) for energies between 2.76 TeV up to 10^9 TeV for the KFK initial conditions

way to allow for the growth of the integrated cross sections is by diffusion for large b. For very large energies the profiles behave as traveling waves and we obtain a geometric scaling [47]; in other words the scattering process becomes function of a single scaled variable $h(s, t)$. Similar property was recently discussed in [48,49]. Another important observation on the inelastic profile is the existence of a toroidal-like structure [50], later dubbed as 'hollowness' effect [51], which was also studied in subsequent works [36,52,53]. In Fig. 3 we observe this effect starting from 13 TeV and it seems to persist for larger energies.

4 Summary

Elastic scattering of hadrons is one of the most basic processes, yet it is incredibly rich in complicated dynamics, which is still not completely understood. In the present work we change radically the way one can approach this fundamental problem applying an evolution equation for complex amplitudes. The equation has its origin in dynamics of Pomeron interactions and has the potential to include the Odderon field plus higher order interaction terms. Using realistic models as initial conditions we describe the Large

Hadron Colider data in a broad kinematic range and we are able to extrapolate our predictions to cosmic ray energies.

Data Availability Statement This manuscript has no associated data or the data will not be deposited. [Authors' comment: This is theoretical/phenomenological work and no data was generated or processed.]

References

1. S. Donnachie, G. Dosch, P. Landshoff, O. Nachtmann, *Pomeron Physics and QCD, Cambridge Monographs on Particle Physics, Nuclear Physics and Cosmology* (Cambridge University Press, Cambridge, 2002)
2. V.S. Fadin, E. Kuraev, L. Lipatov, Phys. Lett. B **60**, 50 (1975)
3. E.A. Kuraev, L.N. Lipatov, V.S. Fadin, Sov. Phys. JETP **45**, 199 (1977) [Zh. Eksp. Teor. Fiz.72, 377 (1977)]
4. I.I. Balitsky, L.N. Lipatov, Sov. J. Nucl. Phys. **28**, 822 (1978) [Yad. Fiz. 28, 1597 (1978)]
5. J.R. Forshaw, D.A. Ross, *Quantum Chromodynamics and the Pomeron*, vol. 9 (Cambridge University Press, Cambridge, 2011)
6. L.V. Gribov, E.M. Levin, M.G. Ryskin, Phys. Rep. **100**, 1 (1983)
7. I. Balitsky, Nucl. Phys. B **463**, 99 (1996). arXiv:hep-ph/9509348
8. Y.V. Kovchegov, Phys. Rev. D **60**, 034008 (1999). arXiv:hep-ph/9901281
9. C. Marquet, R.B. Peschanski, G. Soyez, Nucl. Phys. A **756**, 399 (2005). arXiv:hep-ph/0502020
10. J. Jalilian-Marian, A. Kovner, A. Leonidov, H. Weigert, Nucl. Phys. B **504**, 415 (1997). arXiv:hep-ph/9701284
11. J. Jalilian-Marian, A. Kovner, A. Leonidov, H. Weigert, Phys. Rev. D **59**, 014014 (1998). arXiv:hep-ph/9706377
12. J. Jalilian-Marian, A. Kovner, H. Weigert, Phys. Rev. D **59**, 014015 (1998). arXiv:hep-ph/9709432
13. A. Kovner, J.G. Milhano, H. Weigert, Phys. Rev. D **62**, 114005 (2000). arXiv:hep-ph/0004014
14. A. Kovner, J.G. Milhano, Phys. Rev. D **61**, 014012 (2000). arXiv:hep-ph/9904420
15. H. Weigert, Nucl. Phys. A **703**, 823 (2002). arXiv:hep-ph/0004044
16. E. Iancu, A. Leonidov, L.D. McLerran, Nucl. Phys. A **692**, 583 (2001). arXiv:hep-ph/0011241
17. E. Ferreiro, E. Iancu, A. Leonidov, L. McLerran, Nucl. Phys. A **703**, 489 (2002). arXiv:hep-ph/0109115
18. H. Navelet, S. Wallon, Nucl. Phys. B **522**, 237 (1998). arXiv:hep-ph/9705296
19. C. Ewerz, The perturbative pomeron and the odderon: where can we find them? (2004). arXiv:hep-ph/0403051
20. K.J. Golec-Biernat, A.M. Stasto, Nucl. Phys. B **668**, 345 (2003). arXiv:hep-ph/0306279
21. E. Gotsman, E. Levin, Phys. Rev. D **101**, 014023 (2020)
22. V. Gribov, *Strong Interactions of Hadrons at High Energies: Gribov Lectures on Theoretical Physics, Cambridge Monographs on Particle Physics, Nuclear Physics and Cosmology* (Cambridge University Press, Cambridge, 2008)
23. V.N. Gribov, Zh. Eksp, Teor. Fiz. **53**, 654 (1967)
24. H.D. Abarbanel, J.D. Bronzan, R.L. Sugar, A.R. White, Phys. Rep. **21**, 119 (1975)
25. D. Amati, L. Le Bellac, G. Marchesini, M. Ciafaloni, Nucl. Phys. B **112**, 107 (1976)
26. V. Allesandrini, D. Amati, R. Jengo, Nucl. Phys. B **108**, 425 (1976)
27. V. Alessandrini, D. Amati, M. Ciafaloni, Nucl. Phys. B **130**, 429 (1977)
28. R.A. Fisher, Ann. Eugen. **7**, 355 (1937). https://doi.org/10.1111/j.1469-1809.1937.tb02153.x
29. A. Kolmogorov, I. Petrovsky, N. Piscounov, Moscou Univ. Bull. Math. A **1**, 1 (1937)
30. S. Munier, R.B. Peschanski, Phys. Rev. Lett. **91**, 232001 (2003). arXiv:hep-ph/0309177
31. V.M. Abazov et al., TOTEM, D0, Phys. Rev. Lett. **127**, 062003 (2021). arXiv:2012.03981 [hep-ex]
32. R. Peschanski, Phys. Rev. D **79**, 105014 (2009)
33. A.K. Kohara, E. Ferreira, T. Kodama, Eur. Phys. J. C **74**, 3175 (2014). arXiv:1408.1599 [hep-ph]
34. C. Bourrely, J. Soffer, T.T. Wu, Phys. Rev. D **19**, 3249 (1979)
35. Y.V. Kovchegov, L. Szymanowski, S. Wallon, Phys. Lett. B **586**, 267 (2004). arXiv:hep-ph/0309281
36. E. Ferreira, A.K. Kohara, T. Kodama, Eur. Phys. J. C **81**, 290 (2021). https://doi.org/10.1140/epjc/s10052-021-09056-1
37. P. Zyla et al. (Particle Data Group), PTEP **2020**, 083C01 (2020), and 2021 update
38. D. Amati, L. Caneschi, R. Jengo, Nucl. Phys. B **101**, 397 (1975)
39. O.V. Selyugin, Phys. Rev. D **91**, 113003 (2015)
40. T. Csorgo, I. Szanyi, Eur. Phys. J. C **81**, 611 (2021). arXiv:2005.14319 [hep-ph]
41. A. Martin, Phys. Lett. B **404**, 137 (1997)
42. T. Csörgő, I. Szanyi, in *International Scientific Days—Femtoscopy Session* (2022). https://indico.cern.ch/event/1152630/
43. G. Antchev et al. (The TOTEM Collaboration), First measurement of elastic, inelastic and total cross-section at $\sqrt{s} = 13$ tev by totem and overview of cross-section data at lhc energies (2017)
44. P. Abreu et al., The Pierre Auger Collaboration, Phys. Rev. Lett. **109**, 062002 (2012)
45. G.A. et al. (ATLAS Collaboration), Nucl. Phys. B **889**, 486 (2014)
46. M.A. et al. (ATLAS Collaboration), Phys. Lett. B **761**, 158 (2016)
47. A.J. Buras, J. Dias de Deus, Nucl. Phys. B **71**, 481 (1974)
48. T. Csörgő, T. Novak, R. Pasechnik, A. Ster, I. Szanyi, Eur. Phys. J. C **81**, 180 (2021). arXiv:1912.11968 [hep-ph]
49. C. Baldenegro, C. Royon, A.M. Stasto, Phys. Lett. B **830**, 137141 (2022). arXiv:2204.08328 [hep-ph]
50. I.M. Dremin, Phys. Usp. **58**, 61 (2015)
51. E. Arriola, W. Broniowski, Few-Body Syst. **57**, 485–490 (2016). arXiv:1602.00288
52. T. Csörgő, R. Pasechnik, A. Ster, Eur. Phys. J. C **80**, 126 (2020). https://doi.org/10.1140/epjc/s10052-020-7681-8

53. J. Procházka, V. Kundrát, Eur. Phys. J. C **80**, 779 (2020). https://doi.org/10.1140/epjc/s10052-020-8334-7
54. G. Antchev et al. (The TOTEM Collaboration), Eur. Phys. J. C **80**, 91 (2020). https://doi.org/10.1140/epjc/s10052-020-7654-y
55. G. Antchev et al. (TOTEM collaboration), EPL **101**, 21002 (2012)
56. G. Antchev et al., TOTEM, Eur. Phys. J. C **76**, 661 (2016). arXiv:1610.00603 [nucl-ex]
57. G. Antchev et al., TOTEM Collaboration. Eur. Physi. J. C **79**, 861 (2019). https://doi.org/10.1140/epjc/s10052-019-7346-7
58. G. Antchev et al., TOTEM, Eur. Phys. J. C **82**, 263 (2022). arXiv:2111.11991 [hep-ex]